Laser-induced anisotropy near a focus

1999 J. Phys.: Condens. Matter 11 7377

(http://iopscience.iop.org/0953-8984/11/38/315)

J. Phys.: Condens. Matter **11** (1999) 7377–7383. Printed in the UK PII: S0953-8984(99)03626-7

Laser-induced anisotropy near a focus

X Chen and H Berger

Laboratoire de Physique de l'Université de Bourgogne, 9, Avenue A Savary, BP 47 870, 21078 Dijon Cédex, France

Received 28 April 1999

Abstract. Optically isotropic materials may become anisotropic when illuminated by a strong laser beam. The induced anisotropy is proportional to the beam intensity, and it produces a depolarization of the laser beam. If the material is placed near the beam focus, usually the induced depolarization is strong due to the high beam intensity. We observed that in terbium gallium garnet, however, the induced depolarization is reduced sharply near the focus. It presents a minimal dip at this position. This phenomenon was not observed previously. In our analysis, we show that the refractive index variations in both transverse and longitudinal directions contribute to the phase shift responsible for the depolarization. As a result, the observed dip is closely related to the beam divergence. The competition between these two contributions plays a key role in the polarization changes near the focus.

1. Introduction

Laser-induced depolarization is one of the nonlinear optical effects which accompanies the self-focusing effect [1]. When an isotropic absorbing crystal is placed between two crossed polarizers and is illuminated with an intense light beam, one observes a characteristic interference pattern. It is also called a conoscopic pattern [2]. Its origin is the thermal stress birefringence. In most applications, this pattern has a disturbing harmful effect [3,4]. However, recent works show that it may become useful [5]. For example, such patterns can be used in material characterizations [6] and in vectorial sensing [7]. Although the self-focusing phenomenon near the laser beam focus has been extensively studied, reports on the induced depolarization behaviour near the focus are not numerous. In particular, only few data concern materials other than laser materials. Our investigation on terbium gallium garnet, which is a typical magneto-optical material, revealed an unusual polarization change. Our experimental observation is interpreted through a new analytical description of the laser-induced conoscopic pattern. We will show that the evolution of this pattern near the focus region provides useful knowledge on the relative change of the refractive index components induced by laser.

2. Experiment

A naturally isotropic crystal $Tb_3Ga_5O_{12}$ is illuminated with a cw argon-ion laser operated at the crystal absorption resonance at $\lambda = 488$ nm as described in reference [8]. The beam waist size w is focused using a focusing lens of $f = 50$ mm. The beam power (P) is varied with a half-wave plate and a polarizer combination. Suppose that the beam propagates along the z-axis. A parallel-plane cylindrical sample with radius $r_0 = 5$ mm and thickness $L = 5$ mm is mounted on a longitudinal (parallel to the beam propagation direction) translation stage, placed

0953-8984/99/387377+07$30.00

between crossed polarizers. We denote the first and second polarizer's polarization axes as x and y respectively. Behind the second polarizer, a digital camera captured the pattern intensity $I(r, \phi)$, where r and ϕ are the usual cylindrical coordinates. The digitized pixel intensities of the images were stored and processed on a computer. To measure the total intensity of the pattern, a photodiode replaced the camera. The signal collected by the photodiode, I_{exp}, is recorded on a digital oscilloscope. We denote the longitudinal distance between the sample entrance face and the lens as z. We observed that the image intensity is very weak when the sample is placed at $z = 49.4$ mm. Let us take $z^* = z - 49.4$ mm as a relative sample position. The laser-induced intensity distributions $I(r, \phi)$ near the focus, for (a) $z^* = 0$, (b) $z^* = 1$ mm and (c) $z^* = 4$ mm are shown in figure 1. We observed that the intensity $I(r, \phi)$ increases from (a) to (b), then decreases from (b) to (c). The intensity I_{exp} measured by the photodiode by scanning the sample near the focus is shown in figure 2, where the points (a), (b) and (c) correspond to the three patterns in figure 1. The intensity presents a clear narrow minimum at $z^* \approx 0$. The width of this dip is about 1.6 mm. By fluorescence monitoring [9], one can easily see that the dip occurs when the new focus inside the sample coincides with the sample longitudinal centre. To determine the z-position of the dip quantitatively, a Z-scan

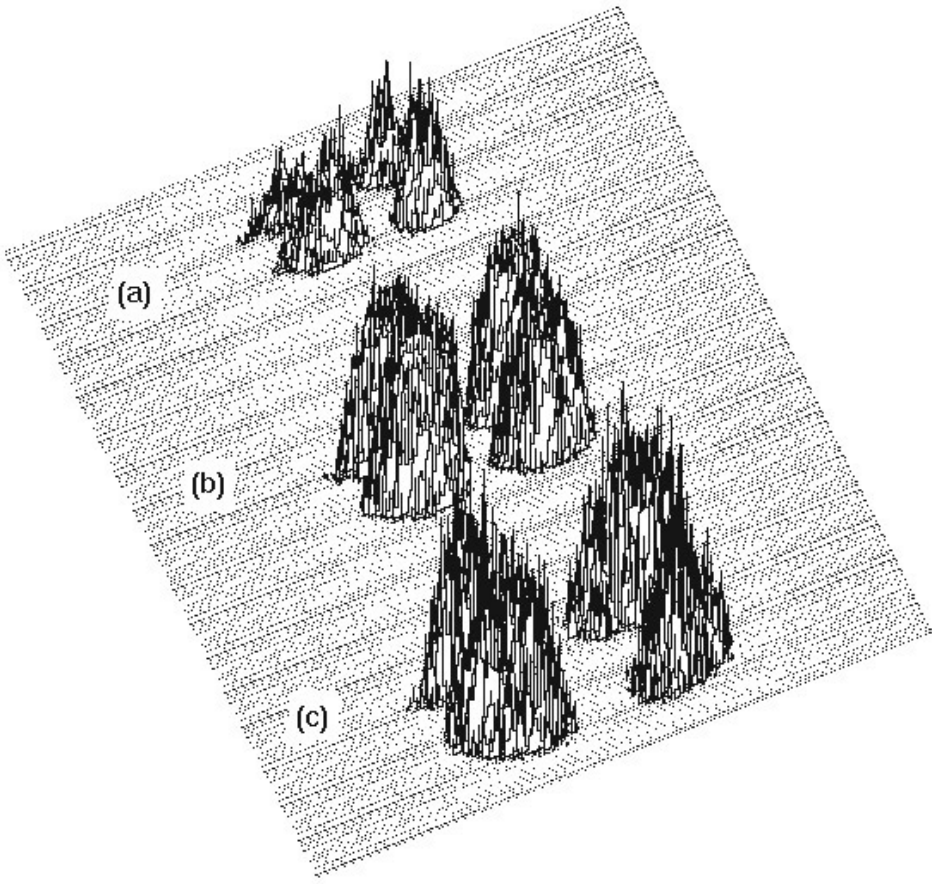

Figure 1. The measured spatial intensity distribution $I(r, \phi)$ for different sample positions. (a) $z^* = 0$; (b) $z^* = 1$ mm; (c) $z^* = 4$ mm.

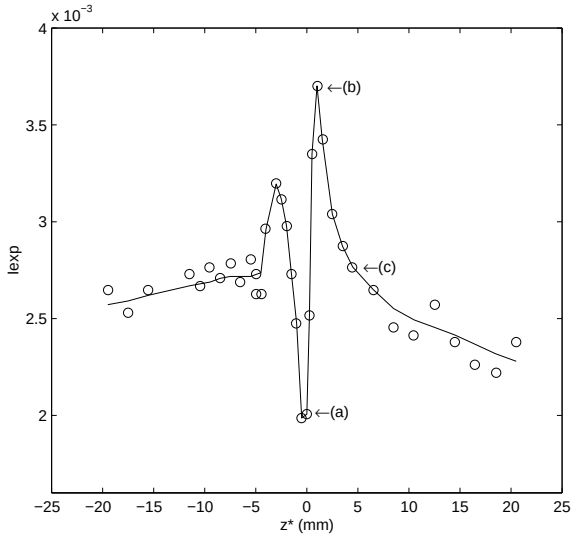

Figure 2. The measured intensity I_{exp} obtained by scanning the sample near the focus, showing a dip. (a), (b) and (c) correspond to the positions used in figure 1 and figure 3. The solid line is a guide to the eye.

technique [9] is used. We denote the front point as z_f; it is the z-position where the focus coincides with the entrance face. z_r is the rear point; it is the z-position where the focus coincides with the exit face. Experimentally, the Z-scan shows that the dip occurs right at the middle between these two points.

3. Analysis

Theoretically, the clearest and the most detailed analysis of laser-induced thermal stress birefringence in cw operation is given in [2]. For a cylindrical sample under the assumption of uniform internal heat generation per unit volume Q and strictly radial heat flow, the steady-state heat equation leads to a parabolic temperature profile with the highest temperature at the centre of the rod [10]:

$$T(r) = T(r_0) + \frac{Q}{4K}(r_0^2 - r^2) \tag{1}$$

where K is the thermal conductivity and r_0 is the sample radius. The temperature gradients generate mechanical stresses. In an isotropic rod, according to this temperature distribution, the radial, tangential and axial stresses are parabolic functions of r. The stresses generate thermal strains which in turn produce refractive index variations via the photoelastic effect. Since the transverse stresses are in radial and tangential directions, the local indicatrix also orients its axis in these directions (n_r and n_ϕ). In the transverse direction, the induced birefringence is then [2, 11, 12]

$$\Delta n_r - \Delta n_\phi = \frac{\alpha Q}{K} n_0^3 C_B r^2 \tag{2}$$

where C_B is a material parameter, including the elasto-optical coefficients, n_0 is the linear refractive index and α is the thermal expansion coefficient. For a Gaussian-type heat generation, the temperature and refractive index distributions near the beam axis are very similar [6, 13].

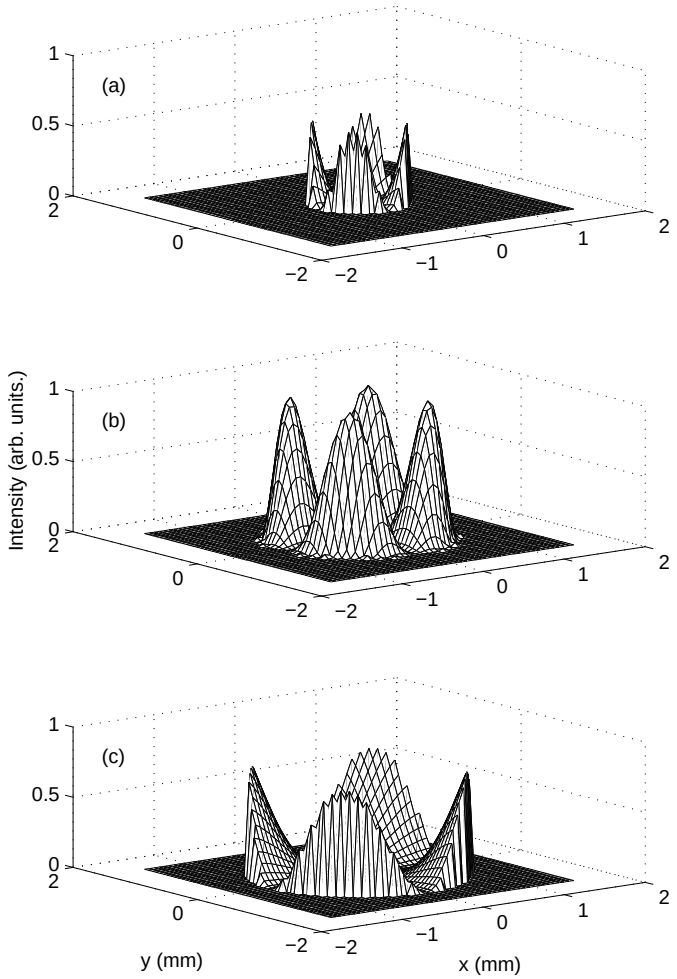

Figure 3. The calculated spatial intensity distributions $I(r, \phi)$ for sample positions (a), (b) and (c).

A linearly polarized beam passing through the sample will experience a phase difference $\delta(r)$ between the two components along Δn_r and Δn_ϕ: $\delta(r) = (2\pi L/\lambda)(\Delta n_r - \Delta n_\phi)$. Hence a polarization change at each point of the transverse section yields a spatial elliptical polarization pattern, except for points located along the x-axis (the polarizer's axis) and y-axis, where the polarization remains linear. If one places an analyser with its axis oriented perpendicularly to the initial polarization, then the transmitted intensity becomes

$$I(\phi, r) = I_0 \mathrm{e}^{-bL} \sin^2(2\phi) \sin^2 \frac{\delta(r)}{2} \tag{3}$$

where I_0 is the incident intensity, b is the absorption coefficient and ϕ is the angle with respect to that of the initial polarization. Usually this description is sufficient for interpreting the experimental results. In our experiment, the changes of the beam size make the interpretation more delicate. Since the heat generation Q is proportional to the beam intensity P/w^2, equation (2) implies that if the beam size w is reduced, the birefringence $\Delta n_r - \Delta n_\phi$ increases. At the beam focus, as the beam size reduces to a minimum, one expects a maximal intensity

$I(\phi, r)$, if $\Delta n_r - \Delta n_\phi$ is the unique contribution to the phase difference, while our observation of a minimal dip rather than a maximal peak at the focus suggests an additional contribution to the phase shift. According to our analysis, this additional contribution is due to the refractive index change along the z-axis. Indeed, such a change has been studied in [11]:

$$n_z - n_y = a + br^2 \tag{4}$$

where $a = \frac{8}{3}Sp_{44}$ and $b = -2S(p_{11} - p_{12})(\nu + 1) - Sp_{44}(\frac{2}{3}\nu + 6)$, the p_{ij} are the elasto-optical coefficients of the material, ν is Poisson's ratio and

$$S = \frac{n_0^3 \alpha Q r_0^2}{32K(1-\nu)}.$$

As indicated in reference [11], locally the crystal becomes biaxial ($n_x(r) \neq n_y(r) \neq n_z(r)$). This means that there exist two optical axes at any point in the sample (symmetric with each other about the z-axis). Let us consider an arbitrary point in the transverse plane of the sample which is at a distance r from the z-axis. We denote by β the angle that each optical axis makes with the z-axis and by θ the angle made by a wave normal, $\vec{s}$, with the z-axis. Fresnel's equation of wave normals leads to two solutions. One of them has velocity $\vec{v'}$, the other $\vec{v''}$. The two speeds are related by the following relation [14]:

$$v'^2 - v''^2 = (v_x^2 - v_y^2)\sin\theta_1 \sin\theta_2 \tag{5}$$

where θ_1 and θ_2 are the angles between $\vec{s}$ and each optical axis defined by $\theta_1 = \theta - \beta$ and $\theta_2 = \theta + \beta$. This implies that

$$\sin\theta_1 \sin\theta_2 = \left(\frac{r}{\rho}\cos\beta\right)^2 - \left(\frac{L}{\rho}\sin\beta\right)^2 \tag{6}$$

where $\rho = \sqrt{r^2 + L^2}$, and the angle β is related to the velocity components:

$$\tan^2\beta = \frac{v_x^2 - v_y^2}{v_y^2 - v_z^2}. \tag{7}$$

Using $v = c/n$, one has the result

$$\frac{1}{n'^2} - \frac{1}{n''^2} = \sin^2\theta\left(\frac{1}{n_y^2} - \frac{1}{n_z^2}\right) - \cos^2\theta\left(\frac{1}{n_x^2} - \frac{1}{n_y^2}\right). \tag{8}$$

Since the differences between the refractive indices are small compared with their values, the transmitted intensity in equation (3) becomes

$$I(r,\phi) = I_0 e^{-\beta L}\sin^2(2\phi)\sin^2\frac{\pi L}{\lambda}[(n_z - n_y)\sin^2\theta - (n_y - n_x)\cos^2\theta]. \tag{9}$$

The $n_y - n_x$ term is nothing but the stress birefringence evaluated in the plane perpendicular to the z-axis; it corresponds to $\Delta n_\phi - \Delta n_r$ in a cylindrical coordinate system. The $n_z - n_y$ term is new compared with the usual theoretical considerations in laser-induced thermal birefringence. Due to the Q-dependence, both $n_y - n_x$ and $n_z - n_y$ are linear functions of $1/w^2$. Equation (9) appears now as the general equation describing the transmitted intensity. Let us consider its different applications.

(1) *Far from the focus.* Using a Gaussian-type beam, if the sample is positioned outside the Rayleigh range, θ is nearly a constant: $\theta \simeq \theta_{max} = \lambda/(\pi n_0 w_0)$ [15]. It is of the order of 9 mrad in our experiment. Owing to the dependence on $1/w^2$ of both $n_y - n_x$ and $n_z - n_y$, one finds naturally that $I(r,\phi)$ decreases with increasing w. This result is in good agreement with figure 2.

(2) *Near the focus.* In the vicinity of the focus, i.e. in the Rayleigh range of a Gaussian-type beam, the angle θ is evaluated from the derivative of the waist versus z. It is smaller than θ_{max} and is z-dependent. Consequently, as one approaches the minimal waist point (w_0), the intensity $I(r, \phi)$ may increase or decrease as a result of the competition between the terms in θ and in $1/w^2$. In the following, we define $R = |n_y - n_x|/|n_z - n_y|$, and we discuss two cases.

   (a) $R = |n_y - n_x|/|n_z - n_y| \gtrsim \tan^2\theta$. In this case the $n_y - n_x$ term in the bracket dominates. Due to the dependences on both $\cos^2\theta$ and $1/w^2$, as one approaches the focus, $I(r, \phi)$ increases. Thus a peak is expected around w_0.

   (b) $R = |n_y - n_x|/|n_z - n_y| < \tan^2\theta$. In this case, the $n_z - n_y$ term in the bracket dominates. Comparing to the theory of the uniaxial crystal, we find the well-known term $(n_e - n_o)\sin^2\theta$ in the phase difference between the ordinary wave and the extraordinary wave in a uniaxial crystal [14], by identifying $n_z = n_e$ and $n_y \approx n_x = n_o$. This means that the nonlinear medium behaves like a uniaxial crystal [16]; the equivalent optical axis is along the z-axis. Near the focus, the terms in $\sin^2\theta$ and $1/w^2$ contribute destructively to $I(r, \phi)$. This explains why the measured pattern intensity decreases when the sample approaches w_0 (from (b) to (a) in figure 1). In the case of an ideal uniaxial crystal, $n_y - n_x = 0$, when θ reduces to zero at w_0 (parallel beam), $I(r, \phi) = 0$, yielding a minimal dip with null intensity. However, if $n_y - n_x$ is small but not zero, $I(r, \phi)$ reduces to a finite minimum. This is the case observed in our experiment. The numerical results for $R = 3 \times 10^{-6}$ are shown in figure 3.

(3) *With a parallel beam.* The angle θ reflects the name conoscopic, because 'cono' indicates a cone-like character of the beam [17]. If the beam is parallel, i.e. $\theta = 0$, only the $n_y - n_x$ term contributes to the conoscopic pattern.

(4) *The dip position.* Using the Z-scan technique in the self-focusing model developed in [9], we found a minimum at $z = 49.4$ mm. As $z_f = 50.6$ mm and $z_r = 48.1$ mm (they are separated by $L(1 - 1/n_0)$ [9, 18]), the expected dip lies at the middle between these two points. This is in good agreement with the measurement shown in figure 2.

The above analysis can be used to determine an inequality between the relative changes of the refractive index components induced by the laser. Qualitatively, if a maximal peak of $I(r, \phi)$ is observed at w_0, one knows that $|n_z - n_y| \lesssim |n_y - n_x|$; otherwise, if a minimal dip is observed instead, one knows that $|n_z - n_y| \gg |n_y - n_x|$; finally, if one observes zero intensity at the minimal dip, then one knows that $|\Delta n_z| \neq |\Delta n_y| = |\Delta n_x|$. It would be interesting to develop further investigations in order to quantitatively evaluate the indicatrix change. The knowledge of the latter should provide a method for making measurements of material constants—for example, the elasto-optic coefficients.

4. Conclusions

A narrow dip in the laser-induced conoscopic pattern in terbium gallium garnet has been observed. This observation implies that the beam depolarization is minimal when the sample is placed close to the laser focus. The origin of this effect is found to be the conic character of the beam, and has been interpreted by introducing a new term in the general formula which has been neglected up to now. The actual conoscopic pattern intensity expression is extended to the following formula:

$$I(\phi, r) = I_0 \mathrm{e}^{-bL} \sin^2(2\phi) \sin^2 \frac{\pi L}{\lambda} [(n_z - n_y)\sin^2\theta - (n_y - n_x)\cos^2\theta] \tag{10}$$

in which the index changes in the transverse direction $n_y - n_x$ and in the longitudinal direction $n_z - n_y$ both contribute. Their relative importance can be described by a ratio R ($R = |n_y - n_x|/|n_z - n_y|$). If $R \gtrsim \tan^2\theta$, the depolarization will present a peak, i.e. the beam polarization will be distorted maximally. In contrast, if $R < \tan^2\theta$, the depolarization will present a dip, i.e. the beam initial polarization will have minimal distortion. Using this formalism, we have been able to qualitatively account for our observations; it allows us to establish an inequality between the induced refractive index components. For terbium gallium garnet, we conclude that $|n_z - n_y| \gg |n_y - n_x|$, i.e. the laser-induced anisotropy causes this material to behave like a uniaxial crystal. Further investigations should lead to a quantitative determination of the induced indicatrix.

Acknowledgments

We wish to thank W Koechner and M Remoissenet for very helpful correspondence and discussions. Financial support from the Conseil Régional de Bourgogne is gratefully acknowledged.

References

[1] Shen Y R 1984 *Principles of Nonlinear Optics* (New York: Wiley) pp 314–23
[2] Koechner W 1996 *Solid-State Laser Engineering* 4th edn (Berlin: Springer) pp 393–409
[3] Eichler H J, Haase A, Menzel R and Siemoneit A 1993 *J. Phys. D: Appl. Phys.* **26** 1884–91
[4] Cerullo G, De Silvestri S, Magni V and Svelto O 1993 *Opt. Quantum Electron.* **25** 489–500
[5] Chen X 1999 *Spatio-Temporal Structures of Laser-Induced Anisotropy and Applications; SPIE Annual Mtg (18–23 July, Denver, CO)* (Philadelphia, PA: SPIE)
[6] Chen X, Calemczuk R, Salce B, Lavorel B, Akir C and Rajaonah L 1999 *Solid State Commun.* **8** 431–34
[7] Chen X 1999 *Appl. Phys.* A at press
[8] Chen X, Lavorel B, Boquillon J P, Saint-Loup R and Jannin M 1998 *Solid State Electron.* **42** 1765–6
[9] Chen X, Lavorel B, Dreier T, Genetier N, Misserey H and Michaut X 1998 *Opt. Commun.* **153** 301–4
[10] Carslaw H S and Jaeger J C 1990 *Conduction of Heat in Solids* (Oxford: Oxford University Press) pp 188–229
[11] Koechner W and Rice D K 1970 *Quantum Electron.* **6** 557–66
[12] Foster J D and Osterink L M 1970 *J. Appl. Phys.* **41** 3656–63
[13] Gordon J P, Leite R C C, Moore R S, Porto S P S and Whinnery J R 1965 *J. Appl. Phys.* **36** 3–8
[14] Born M and Wolf E 1964 *Principles of Optics* (Oxford: Pergamon) pp 665–718
[15] Yariv A 1991 *Optical Electronics* (New York: Saunders College Publishing) p 49
[16] Chen X and Gonzalez S 1998 *Appl. Phys.* B **67** 611–13
[17] This point has been clarified by Koechner W 1998 private communication
[18] Chapple P B, Staromlynska J and McDuff R G 1993 *J. Opt. Soc. Am.* **11** 975–82